CSIRO PUBLISHING

Functional Plant Biology, 2015, **42**, 746–757
http://dx.doi.org/10.1071/FP15002

Dynamic response of plant chlorophyll fluorescence to light, water and nutrient availability

M. Pilar Cendrero-Mateo[A,B,F,H], *A. Elizabete Carmo-Silva*[C,G], *Albert Porcar-Castell*[D], *Erik P. Hamerlynck*[B], *Shirley A. Papuga*[A,E] *and M. Susan Moran*[B]

[A]Soil Water and Environmental Science, The University of Arizona, 1177 East Fourth Street, Tucson 85721, USA.
[B]USDA Southwest Watershed Research Centre, 2000 East Allen Road, Tucson, AZ 85719, USA.
[C]USDA Arid-Land Agricultural Research Center, 21881 North Cardon Lane, Maricopa, AZ 85138, USA.
[D]Department of Forest Sciences, University of Helsinki, PO Box 27, 00014 Helsinki, Finland.
[E]School of Natural Resources, The University of Arizona, 325 Biosciences East, Tucson, AZ 85721, USA.
[F]Present address: Institute of Bio- and Geosciences, Forschungszentrum Jülich GmbH, Leo-Brandt-Str., 52425 Jülich, Germany.
[G]Present address: Rothamsted Research, Plant Biology and Crop Science, Harpenden, Herts., AL5 2JQ, UK.
[H]Corresponding author. Email: p.cendrero@fz-juelich.de

Abstract. Chlorophyll molecules absorb photosynthetic active radiation (PAR). The resulting excitation energy is dissipated by three competing pathways at the level of photosystem: (i) photochemistry (and, by extension, photosynthesis); (ii) regulated and constitutive thermal energy dissipation; and (iii) chlorophyll-*a* fluorescence (ChlF). Because the dynamics of photosynthesis modulate the regulated component of thermal energy dissipation (widely addressed as non-photochemical quenching (NPQ)), the relationship between photosynthesis, NPQ and ChlF changes with water, nutrient and light availability. In this study we characterised the relationship between photosynthesis, NPQ and ChlF when conducting light-response curves of photosynthesis in plants growing under different water, nutrient and ambient light conditions. Our goals were to test whether ChlF and photosynthesis correlate in response to water and nutrient deficiency, and determine the optimum PAR level at which the correlation is maximal. Concurrent gas exchange and ChlF light-response curves were measured for *Camelina sativa* (L.) Crantz and *Triticum durum* (L.) Desf plants grown under (i) intermediate light growth chamber conditions, and (ii) high light environment field conditions respectively. Plant stress was induced by withdrawing water in the chamber experiment, and applying different nitrogen levels in the field experiment. Our study demonstrated that ChlF was able to track the variations in photosynthetic capacity in both experiments, and that the light level at which plants were grown was optimum for detecting both water and nutrient deficiency with ChlF. The decrease in photosynthesis was found to modulate ChlF via different mechanisms depending on the treatment: through the action of NPQ in response to water stress, or through the action of changes in leaf chlorophyll concentration in response to nitrogen deficiency. This study provides support for the use of remotely sensed ChlF as a proxy to monitor plant stress dynamics from space.

Additional keywords: nitrogen, non-photochemical quenching, photosynthesis, water deficit.

Received 8 January 2015, accepted 21 April 2015, published online 1 June 2015

Introduction

Water and nutrient availability are two critical factors for plant photosynthesis and plant productivity (Tyner and Webb 1946). Early detection of water and nutrient deficit is essential for sustainable crop management. Photosynthesis is strongly affected by variations in any of these factors, providing a good indicator of plant stress (Chaves 1991); however, it is difficult to measure photosynthesis at the field scale for crop management.

Efforts to find a non-invasive measure of plant photosynthesis using remote sensing have had mixed success (Verma *et al.* 1993; Choudhury 2001). Most reflective vegetation indices are not sensitive to rapid changes in plant photosynthesis status that result from common environmental factors such as low or high solar radiation and drought stress. The exception is the photochemical reflectance index (PRI) (Gamon *et al.* 1992). Over short time scales, PRI can track adjustments in photosynthetic capacity by capturing reflectance changes that are induced by rapid biochemical reactions of the xanthophyll cycle, the biochemical mechanism that enhances thermal dissipation of absorbed light energy (Demmig-Adams and Adams 1992). However, over long time scales (i.e. seasonal), PRI is also influenced by slow changes in leaf pigment pools (Stylinski

et al. 2002), which can erode the general relationship between PRI and photosynthesis under severe stress (Porcar-Castell *et al*. 2012).

The emission of plant chlorophyll fluorescence (ChlF) provides a more direct measure of photosynthesis that has not been fully exploited by remote sensing. The principle underlying the use of ChlF as an indicator of plant physiological status is relatively straightforward. Absorbed light energy excites chlorophyll molecules, and de-excitation of this energy is mainly attained through three competing processes: photochemistry (photochemical quenching (PQ)), radiative loss of photons or ChlF, and non-radiative thermal energy dissipation. For practical reasons, thermal energy dissipation is often divided into basal and regulated components, the latter widely addressed as non-photochemical quenching (NPQ) (Fig. 1) (Porcar-Castell 2011). As these three energy dissipation processes compete for excitation energy, changes in one process (e.g. photochemistry) will affect the other two. Hence, by measuring ChlF, we can derive information on NPQ and PQ (or the rate of electron transport through PSII, Fig. 1); which eventually drives the rate of gross photosynthesis (A_{gross}), and by extension, net photosynthesis (A_{net}, Fig. 1) ($A_{net} = A_{gross}$ – respiration – photorespiration) (Porcar-Castell *et al*. 2014). Importantly, although the above parameters can be easily obtained with active fluorometric systems, such as pulse amplitude modulated (PAM) fluorometers; the remote sensing of ChlF is restricted to the passive estimation of the solar-induced fluorescence (SIF). In principle, the SIF signal is proportional to the traditional PAM steady-state chlorophyll fluorescence (F_s) multiplied by the amount of absorbed PAR, where the exact proportionality factor depends on retrieval and excitation wavelengths and other properties of the measurement (Porcar-Castell *et al*. 2014).

Active measurements have been used to better understand the mechanisms that control SIF and its relationship with photosynthesis and plant physiological status (Keck Institute for Space Studies 2013). Several studies assessing physiological plant status using ChlF have examined leaf-level responses based in the variation of steady-state chlorophyll fluorescence (F_s) (Flexas and Medrano 2002; Baker and Rosenqvist 2004). In most of those studies, F_s was normalised by the minimal fluorescence yield in dark-adapted plants, F_0, to control for differences in chlorophyll content, leaf anatomy, or use of different instruments to measure F_s. Flexas and Medrano (2002) reported that F_s/F_0 in plants growing under a constant photosynthetic active radiation (PAR) exhibited a positive relationship with photosynthesis and a negative relationship with NPQ and concluded that changes in F_s were governed by the regulated component of thermal dissipation, NPQ.

The relationship between photosynthesis, NPQ, and F_s changes with water, nutrient and light availability (Rosema *et al*. 1998; Flexas and Medrano 2002). A common method to characterise the acclimation of photosynthesis is to use a portable infrared gas analyser (IRGA) system to conduct light-response curves of A_{net} and fluorescence parameters such as F_s or NPQ. Under low light, photosynthesis is light-limited and A_{net} increases linearly with illumination. At higher light intensities, light absorption increases accordingly but the carbon reactions start to saturate and A_{net} reaches a plateau. The result is that A_{net} displays a hyperbolic relationship with PAR. The inflection point and maximum A_{net} level depend on photosynthetic capacity (Fig. 2*a*, *d*).

Similarly, because NPQ is one of the main mechanisms used by higher plants to cope with excess light, the light response of NPQ reflects the saturation of A_{net}, increasing rapidly when A_{net} becomes saturated (Gilmore 1997; Serôdio and Lavaud 2011). However, the NPQ increase is limited by the intrinsic capacity of the leaf to dissipate excess light as heat. For example, Serôdio and Lavaud (2011) proposed an analytical model for the quantitative description of the light-response curve of NPQ, based on the close dependence of NPQ with the rapidly reversible quenching. They reported that plants grown under high-light conditions develop larger xanthophyll pools, to dissipate more excess light energy, compared with plants grown under low or intermediate light levels (Gilmore 1997; Verhoeven *et al*. 1997; Serôdio and Lavaud 2011). As a result, NPQ is saturated at lower PAR levels in plants grown under intermediate light, compared with plants grown under high light where the response of NPQ to PAR may appear to be linear for the same range of illumination (Fig. 2*b*, *e*).

Accordingly, the dynamics in A_{net} (via its effect on photochemical quenching capacity (PQ)) and NPQ during a light response curve control those of F_s. For example, Rosema *et al*. (1998) described how A_{net}, NPQ, and F_s changed in response to PAR in well watered plants growing under high-light conditions: (i) A_{net}, shows a hyperbolic relationship with

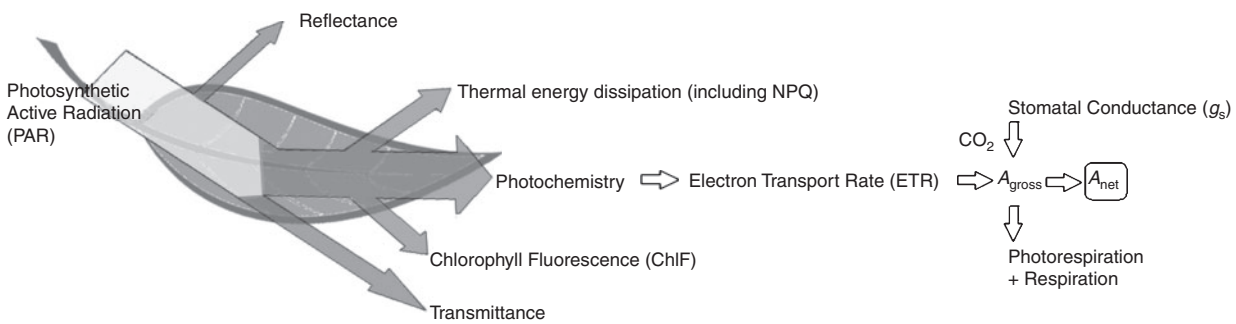

Fig. 1. The fate of incident light in leaves. The absorbed photosynthetically active radiation (PAR) can be dissipated via photochemical electron transport to drive net photosynthesis ($A_{net} = A_{gross}$ – photorespiration – respiration), thermal energy dissipation widely addressed as non-photochemical quenching (NPQ), and chlorophyll fluorescence (ChlF).

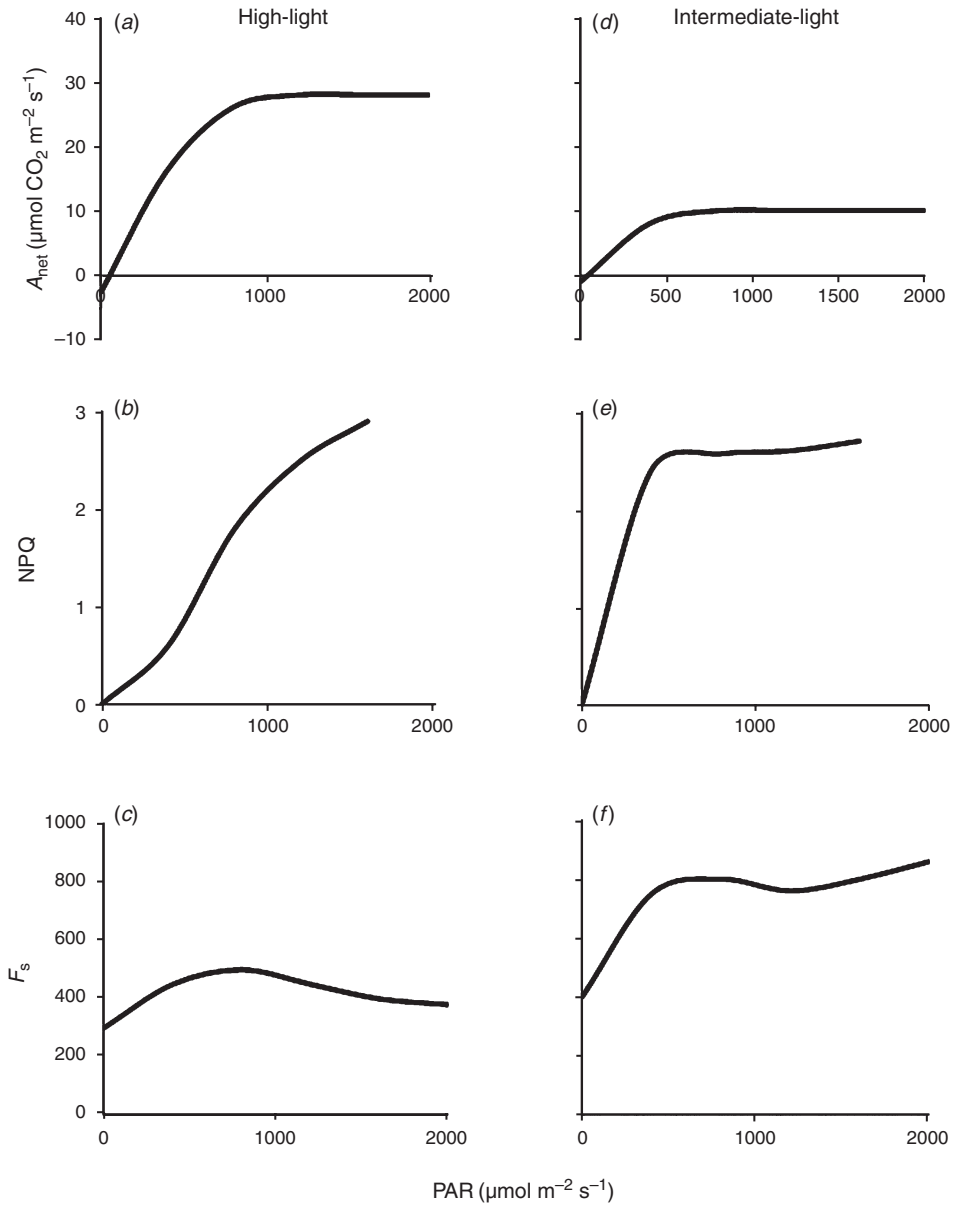

Fig. 2. Representation of net CO_2 assimilation (A_{net}, (*a*, *d*), adapted from Björkman 1981) non-photochemical quenching (NPQ, (*b*, *e*), adapted from Serôdio and Lavaud 2011), steady-state chlorophyll fluorescence (F_s, (*c*, *f*) light-response curves (PAR is photosynthetic active radiation) when plants are grown under (*c*) high theorical estimates, or (*f*) intermediate light conditions, adapted from Flexas and Medrano 2002 and Rosema *et al*. 1998).

PAR, (ii) NPQ shows a rather linear increase with PAR, and thus, (iii) F_s displays two distinctive phases with PAR, increasing at low light (in response to decreasing PQ) and decreasing at high-light (in response to increasing NPQ) (Fig. 2*a–c*). In contrast, for leaves grown under low/intermediate light conditions the response of A_{net} and NPQ to PAR will be hyperbolic, resulting in a different relationship between F_s and PAR relative to leaves grown under high light. We hypothesise that F_s will (i) increase with PAR at low light (in response to decreasing PQ similar to high-light grown leaves); (ii) it will decrease when NPQ increases; and (iii) it will further increase when NPQ reaches saturation (Fig. 2*d–f*).

The amount, quality, and spatiotemporal coverage of SIF data are rapidly increasing. We have a good mechanistic understanding of the short-term process that controls ChlF when plants are exposed to a single stress factor as light, water, or nitrogen (Porcar-Castell *et al*. 2014). However, before using SIF as a reliable indicator of plant photosynthetic status, more work needs to be done to understand the long-term interplay between A_{net} and ChlF when plants are exposed to different sources of stress. We hypothesise that there will be a range of PAR levels for which the dynamics of ChlF and A_{net} over time are directly correlated under the action of NPQ, independent of the light-environment. Accordingly, when

plants with different light growth conditions are exposed to nitrogen or water deficit, we expect that A_{net} and F_s measured under comparable PAR levels will decrease simultaneously under the action of NPQ.

In this study, we investigated the light curves of A_{net}, NPQ, and F_s for plants growing under (i) intermediate light in *Camelina sativa* (L.) Crantz, an oilseed species that is being developed as a source of biofuel (Fröhlich and Rice 2005); and (ii) high light in *Triticum durum* (L.) Desf, one of the most important food sources in the world (Rawson and Gómez Macpherson 2000). An acute stress was induced by water deficit treatment in *Camelina* plants, and a chronic stress was induced by nitrogen treatments in the wheat experiment. The objective of this study was to compare the efficacy of F_s as a proxy for plant stress detection in plants growing under different light environments and different sources of stress; with the final goal of identifying the optimum irradiance level for detecting water and nutrient deficits with ChlF for remote sensing applications.

Materials and methods

Light-response curves of gas exchange and fluorescence

Concurrent light-response curves of gas exchange and fluorescence were measured for *Camelina sativa* (L.) Crantz and *Triticum durum* (L.) Desf plants grown under intermediate-light growth chamber conditions (Experiment I) and high light environment field conditions (Experiment II). Plant stress was induced by withdrawing water in the chamber experiment, and applying different nitrogen levels in the field experiment.

In both Experiment I and Experiment II, gas exchange (net photosynthetic CO_2 assimilation, A_{net} and stomatal conductance to water vapour, g_s) and fluorescence light-response curves were measured using a Li-Cor 6400XT (Li-Cor Biosciences, Lincoln, NE, USA) portable photosynthesis system equipped with a 6400-40 leaf chamber fluorometer with a light source of independently controlled LEDs (three blue, one far-red, and one red, Li-Cor Biosciences). Reference CO_2 concentration was 380 µmol mol^{-1} by mixing CO_2-depleted external air with CO_2 provided from a gas cylinder injection system attached to the photosynthesis system. Leaf temperature was maintained at 25°C, and the enclosed leaf area was 2 cm^2 by ensuring that each leaf filled the entire sample cuvette aperture.

Dark-adapted fluorescence and gas exchange measurements were taken before the beginning of the photoperiod (at 0500 hours) and light-adapted measurements commenced 4 h after the beginning of the photoperiod. All light-adapted measurements were concluded within ~6 h. The same leaf of each plant was analysed for dark- and light-adapted conditions. Light-response curves were generated by varying the incident PAR levels stepwise from 1800, 1200, 800, 500, 300, 200, 100, 50 and 0 µmol m^{-2} s^{-1}. Leaves were allowed to acclimate for 1–4 min at each PAR level; longer acclimation time was usually needed at the lower PAR (i.e. 1, 2, and 3 min for PAR = 1800, 300, and 0 µmol m^{-2} s^{-1} respectively). Measurements were taken when A_{net}, g_s, and internal CO_2 achieve steady-state conditions. Light-response curves in which PAR was increased incrementally from 0 to 1800 µmol m^{-2} s^{-1} were also measured on some of the plants to ensure that the procedure did not induce changes in the parameter magnitudes.

Measured chlorophyll fluorescence parameters included minimal fluorescence in the dark (F_0), F_s, light- and dark-adapted maximal fluorescence (F_m, F_m'), maximum PSII photochemical efficiency (F_v/F_m), and electron transport rate (ETR) (Table 1). Maximum fluorescence yields were achieved by exposing the enclosed leaf to a 2 s flash of saturating light (3000 µmol m^{-2} s^{-1}). Additionally, photochemical (PQ) and non-photochemical (NPQ) excitation quenching capacities where estimated via the fluorescence parameters PQ and NPQ respectively (Table 1). The traditional fluorescence parameter NPQ, as well as PQ, denote the magnitude of the respective rate constant relative to the sum of the first order rate constant of fluorescence emission (k_F) and basal or constitutive thermal dissipation k_D, (Laisk *et al*. 1997; Porcar-Castell *et al*. 2014). For instance, if NPQ = 2, the rate constant associated to NPQ

Table 1. Definitions of pulse-amplitude modulated (PAM) chlorophyll fluorescence parameters used in this study

Parameter	Definition	Formulation	Physiological relevance
F_s	Fluorescence emission yield from light-adapted leaves at steady-state	–	Provides information on photosynthetic performance; it is influenced by many factors (Baker 2008)
F_0, F_0'	Minimal fluorescence from dark- and light-adapted leaves, respectively	–	Level of fluorescence when the primary quinone electron acceptor of PSII (Q_A) is maximally oxidised (all functional PSII centres open) (Baker 2008)
F_m, F_m'	Maximal fluorescence from dark- and light-adapted leaves respectively	–	Level of fluorescence when Q_A is maximally reduced (All functional PSII centres closed) (Baker 2008)
F_v, F_v'	Variable fluorescence from dark- and light-adapted leaves, respectively	$F_v = F_m - F_0$ $F'_m = F'_m - F'_0$	Demonstrate the ability of PSII to perform photochemistry (Q_A reduction) (Baker 2008)
PQ	Photochemical quenching, or relative rate constant of photochemistry	$PQ = \left(\frac{F_m}{F_s} - \frac{F_m}{F'_m}\right)$	Estimates the actual PQ capacity. Note that the parameters PQ and NPQ have the same relative range (Porcar-Castell 2011)
F_v/F_m	Maximum quantum efficiency of PSII	–	Maximum efficiency at which light absorbed by PSII is used for reduction of Q_A
NPQ	Non-photochemical quenching or relative rate constant of regulated thermal dissipation	$NPQ = \frac{F_m}{F'_m} - 1$	Estimates the non-photochemical quenching from F_m to F_m'. Monitors the apparent rate constant for heat loss from PSII (Baker 2008)

(k_{NPQ}) = 2(k_F + k_D), and the same for PQ. The advantage of using PQ instead of the widely used qP or qL parameters (Krause and Weis 1984; Kramer *et al*. 2004) is that PQ is expressed in the same relative units as NPQ, facilitating the quantitative comparison between photochemical and non-photochemical processes (e.g. Fig. 3). Instead, the photochemical quenching parameters qP and qL represent the fraction of open reaction centres for a system without energy transfer between PSII units or with perfect connectivity, respectively, and can each vary between zero and one (Kramer *et al.* 2004; Porcar-Castell *et al.* 2014).

Plant material, growth conditions and experimental design

Experiment I: Intermediate-light history and water deficit

Camelina sativa cv. Robinson plants were grown in a controlled-environment chamber at 25/18°C with a 12 h

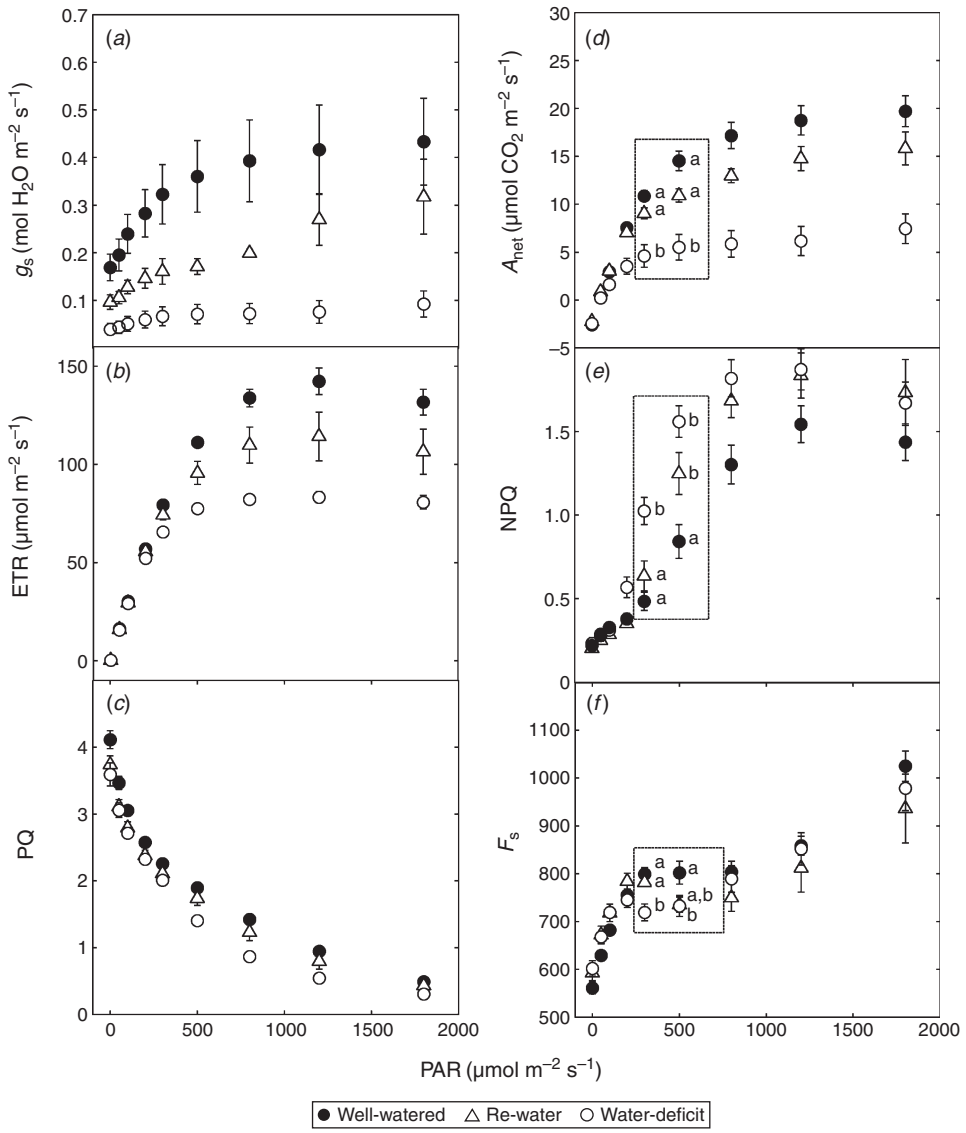

Fig. 3. Experiment I: Intermediate-light history and water deficit. (*a*) Light-response of stomatal conductance (g_s), (*b*) electron transport rate (ETR), (*c*) photochemical quenchin (PQ), (*d*) CO_2 assimilation (A_{net}), (*e*) non-photochemical quenching (NPQ), and (*f*) steady-state chlorophyll fluorescence (F_s) in *Camelina* plants under well-watered conditions (closed circles), after 8 days without watering (water-deficit, open circles), and 1 day after being re-watered (open triangles). Conditions in the chamber of the photosynthesis system were: reference CO_2 concentration = 380 µmol mol^{-1}, PAR = 0–1800 µmol m^{-2} s^{-1} and leaf temperature set to 25°C. Significant differences in A_{net}, F_s and NPQ were observed at the two intermediate PAR levels, 300 and 500 µmol m^{-2} s^{-1}, highlighted by the squares. Different letters denote significant differences at $P \leq 0.05$ (ANOVA). Values are means ± s.e. (n = 4).

photoperiod and PAR of 500 µmol m^{-2} s^{-1}, intermediate-light (IL-grown), at the Arid-Land Agricultural Research Center in Maricopa, Arizona, USA. All plants were grown from seeds in 4-L pots containing a ready-made soil mixture (Sunshine mix#1, Sun Gro Horticulture, Vancouver, Canada). Plants were kept well watered by adding a nutrient solution containing 2 g L^{-1} of 20-20-20 Peters professional water solution fertiliser (Scotts-Sierra Horticultural Products Co., Marysville, OH, USA) and 0.5 mL L^{-1} micronutrient solution of 2 mM $MnCl_2$, 10 mM H_3BO_3, 0.4 mM $ZnSO_4$, 0.2 mM $CuSO_4$, 0.4 mM Na_2MoO_4 and 0.1 mM $NiCl_2$, used at half-strength twice a week.

After 4.5 weeks of plant growth, measurements were taken from well watered control plants, plants exposed to 7 days without watering, and plants that were also exposed to 7 days without watering but were re-watered 1 day before starting the experiment (1 day re-water recovery). Measurements were taken at Day 8 from the beginning of the watering treatments. For this, 12 pots containing one plant each were divided into the three different treatments: well-watered, water-deficit and re-watered. For the control, four pots were kept under well-watered conditions. Drought stress was imposed by withholding water from the other eight pots, starting 3.5 weeks after planting. The day before starting the experiment, four of the eight pots in the drought treatment were re-watered with half-strength nutrient solution (treatment 3, re-watered).

Experiment II: High-light history and nitrogen deficit

We conducted a wheat experiment at the University of Arizona's Maricopa Agricultural Center (MAC) near Maricopa, Arizona, USA over the winter of 2011–2012. Wheat was growing outdoors under high-light conditions (HL-grown). A split plot design with three replicates of *Triticum aestivum* cv. Orita under three nitrogen fertilizer application levels was used for the experiment. Wheat was planted on 9 December 2011 with a row spacing of 19 cm. *Sorghum drummondii* (Steud.) Millsp. & Chase. (Sudan grass) cover crop was grown in the summer of 2010 to remove excess nitrate from the soil. The field was irrigated based on periodic soil moisture measurements and the AZSched irrigation scheduling software (Martin 2007) to ensure the crop was free of drought stress. Nine flood irrigations were applied from early December to the end of April. A total of 710 mm irrigation water was applied through flood irrigation, with individual irrigations varying in amount from 40 to 100 mm. Precipitation amounted to 41 mm for the 2011–12 growing seasons. The soil texture at the site was predominantly sandy loam and sandy clay loam, as determined by textural analysis of soil samples collected after planting. After 129 days of planting, when plants where fully developed, measurements were taken over plants exposed to high, medium, and low nitrogen fertiliser rates (0, 90, and 202 kg ha^{-1} respectively). For this, three samples per nitrogen treatment were taken from a single replicate.

Additionally in Experiment II, leaf chlorophyll contents were estimated from 24 February to 27 April 2012 once a week using spectroscopy techniques (FieldSpec 3 Hi-Res, Analytical Spectral devices (ASD) Inc., Boulder, CO, USA). The chlorophyll index used was the normalised area over reflectance curve (NAOC, Delegido *et al*. 2010). A total of 81 leaves were measured in each nitrogen treatment and the mean values of the 81 leaves were used for this analysis.

Statistical analysis

Statistical analyses were carried out using MATLAB 2011 (MathWorks Inc., Natick, MA, USA) and Statistix ver. 8.0 (Statistical Analytical, Tallahassee, FL, USA). Values presented in the manuscript are means ± s.e. of all measurements taken for each water and nitrogen regime (n as indicated). Linear regressions of A_{net} against F_s were fitted across all PAR levels to determine the overall relationship between A_{net} and F_s, using an F-test to test if slopes and intercepts differed between treatments (linear regression, Statistix, Statistical Analytical). If slopes were found to differ, pair-wise slope comparisons were made using Tukey's test honestly significant difference (HSD), with HSD exceeding 3.34 considered significant ($P \leq 0.05$; Zar 1974). Differences in g_s, A_{net}, ETR, F_s, F_0, F_s/F_0, F_v/F_m, PQ and NPQ between plants in the different treatments and light level (0, 50, 100, 200, 300, 500, 800, 1200 and 1800 µmol m^{-2} s^{-1} incident PAR) were tested using one-way analysis of variance (ANOVA, Statistix, Statistical Analytical).

Results

Light-response of fluorescence and gas-exchange parameters

A common tendency for the light-response curves of gas-exchange and fluorescence was found in both experiments and treatments (Figs 3, 4) (i) g_s, ETR and A_{net} reached a plateau when PAR >500 µmol m^{-2} s^{-1}, (ii) under rising PAR, PQ declines and NPQ increase, and (iii) since $F_s = F_m(1 + NPQ)/(1 + PQ + NPQ)$ when PQ + NPQ increases, F_s decreases (Porcar-Castell *et al.* 2014). A more detailed explanation of the light-response curves of gas exchange and fluorescence is presented in the following sections.

Experiment I: Intermediate-light history and water deficit

Camelina plants under water deficit had decreased rates of stomatal conductance and photosynthesis (Fig. 3*a*, *d*). Plants that had been re-watered showed signs of recovery of their photosynthetic capacity, but recovery to the level of control values was not completed in 1 day (Fig. 3*d*). Notably, water deficit decreased the maximum photosynthetic rate. For three water treatments, ETR increased whereas PQ decreased with PAR (Fig. 3*b*, *c*). It is important to note that for *Camelina* plants, a significant difference between water treatments for ETR and PQ was observed when the PAR reached the light level at which plants were grown, 500 µmol m^{-2} s^{-1}, and ETR slightly decreased when PAR reached 1800 µmol m^{-2} s^{-1}.

The NPQ and F_s light curves from PAR 0 to 500 µmol m^{-2} s^{-1} (Fig. 3*e*, *f*) in IL-grown *Camelina* showed a complex response to light: (i) at low PAR levels (0–300 µmol m^{-2} s^{-1}) NPQ increased only slowly whereas F_s increased steeply along with decreasing PQ; (ii) at intermediate PAR levels (300–500 µmol m^{-2} s^{-1}) NPQ showed an abrupt increase whereas A_{net} started to show signs of saturation, with F_s remaining rather stable; (iii) when PAR exceeded the light

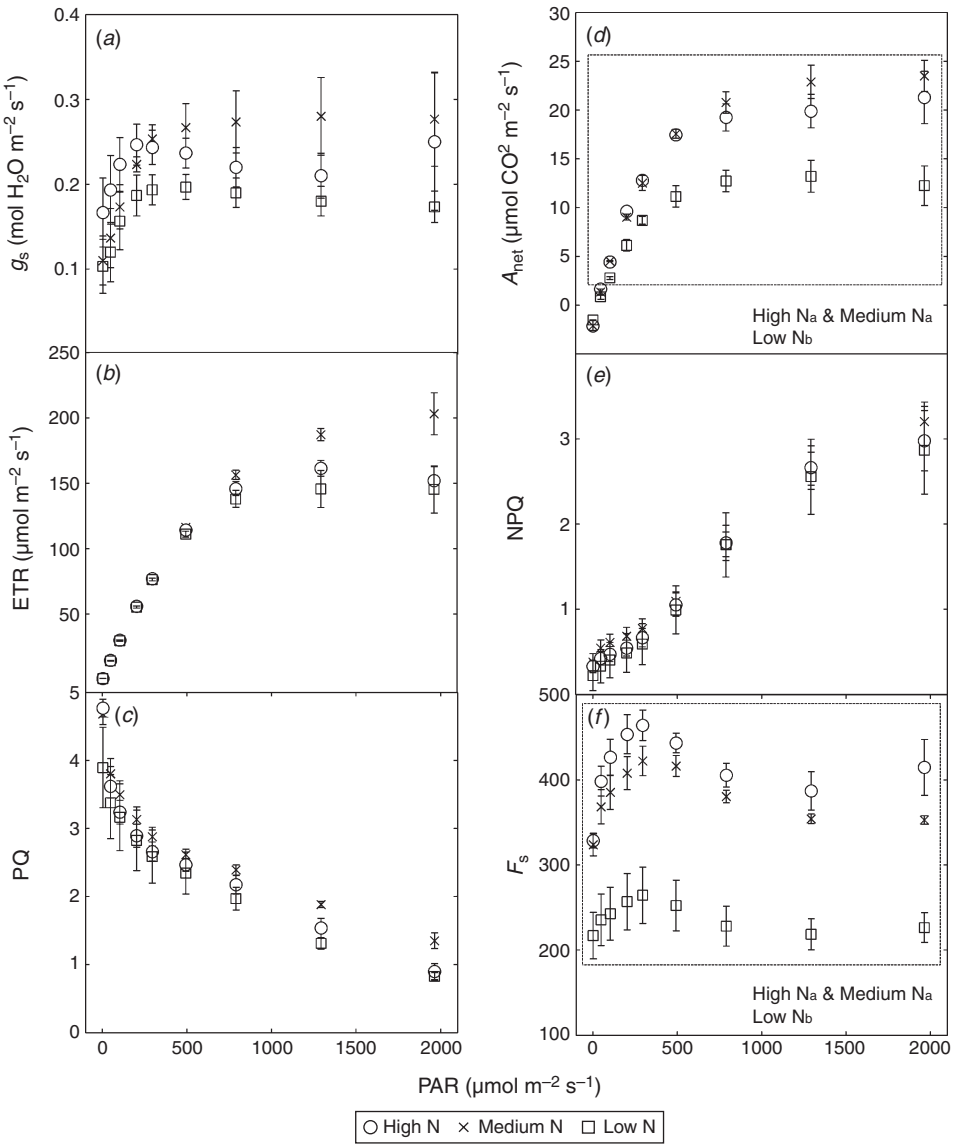

Fig. 4. Experiment II: High-light history and nitrogen deficit. (*a*) Light-response of stomatal conductance (g_s), (*b*) electron transport rate (ETR), (*c*) photochemical quenching (PQ), (*d*) CO_2 assimilation (A_{net}), (*e*) non-photochemical quenching (NPQ), and (*f*) steady-state chlorophyll fluorescence (F_s) in wheat plants under high-nitrogen (open circles), medium-nitrogen (cross), and low-nitrogen conditions (open square). Conditions in the chamber of the photosynthesis system were: reference CO_2 concentration = 380 µmol mol^{-1}, PAR = 0–1800 µmol m^{-2} s^{-1} and leaf temperature set to ambient temperature. Significant differences in A_{net} and F_s were observed from PAR 100 to 1800 µmol m^{-2} s^{-1}, highlighted by the squares. Different letters denote significant differences at $P \leq 0.05$ (ANOVA). Values are means ± s.e. ($n = 3$).

level at which plants were grown (500 µmol m^{-2} s^{-1}), NPQ reached saturation and F_s continued to increase along with decreasing PQ (Fig. 3*c*, *e*, *f*).

It is important to note that no significant effect of watering treatment was observed for F_s when PAR was lower than 300 µmol m^{-2} s^{-1} and higher than 500 µmol m^{-2} s^{-1}. However, between PAR 300 and 500 µmol m^{-2} s^{-1}, F_s in plants exposed to the water deficit and re-water treatments decreased driven by the drastic increase of NPQ (Fig. 3*e*, *f*).

From the *Camelina* light response (Fig. 3), it was apparent that there were significant differences in A_{net}, F_s, and NPQ at the intermediate PAR level that was used for plant growth (300–500 µmol m^{-2} s^{-1}).The average values of A_{net}, F_s and NPQ for each watering treatment at the two intermediate PAR levels, 300 and 500 µmol m^{-2} s^{-1}, are highlighted by the squares in Fig. 3*d–f*. There was a consistently significant difference between the values of all three parameters for the plants under well-watered and water-deficit conditions. The pattern was less consistent for the re-watered plants; i.e. after 1 day of re-watering at PAR = 500 µmol m^{-2} s^{-1}, F_s was not significantly different for the re-watering treatment from the well-watered or water-deficit treatments.

Experiment II: High-light history and nitrogen deficit

Wheat plants under nitrogen deficit had decreased photosynthetic rates and lower stomatal conductance with increasing PAR compared with the other nitrogen-treatments (Fig. 4*a*, *d*). Plants receiving medium fertilizer applications showed higher photosynthetic and stomatal conductance than plants under high nitrogen treatment, when PAR >300 µmol m^{-2} s^{-1} (Fig. 4*d*). Like *Camelina*, ETR increased whereas PQ decreased with PAR (Fig. 4*b*, *c*). However, unlike *Camelina*, no difference between treatments for ETR and PQ was found for wheat, which was grown in an open field under HL. In both experiments, ETR slightly decreased when PAR reach 1800 µmol m^{-2} s^{-1}.

The NPQ and F_s light-curve shapes from PAR 0 to 500 µmol m^{-2} s^{-1} for HL-grown wheat were similar to those for IL-grown *Camelina* (Fig. 4*e*, *f*). Nevertheless, NPQ saturated at much higher PAR in wheat than in *Camelina* (1800 vs 500 µmol m^{-2} s^{-1}). As a result, F_s continued to decline in wheat until PAR = 1800 µmol m^{-2} s^{-1}.

In contrast, nitrogen deficit did not affect NPQ for wheat, no significant difference between treatments was found (Fig. 4*e*). However, nitrogen deficit limited chlorophyll, as indicated by the different magnitudes in chlorophyll content, F_0, and F_s between treatments. NAOC chlorophyll index equalled 0.33, 0.36 and 0.37 for low, medium, and high nitrogen, respectively, with low nitrogen treatment NAOC levels significantly lower from the rest ($n = 9$, $P = 0.05$). F_0 equalled 555, 573, and 585 for low, medium and high nitrogen respectively.

Significant differences in A_{net}, and F_s, were observed over a broader PAR range (PAR = 100–1800 µmol m^{-2} s^{-1}) for HL-grown wheat (Fig. 4*d*, *f*, outlined by squares). A consistent and significant difference between low and both medium and high nitrogen treatments was observed for A_{net}, and F_s. However, no difference between high and medium nitrogen treatments was found either for A_{net} or F_s. Importantly, normalising F_s by F_0 (F_s/F_0) did not improve the results observed either for the water nor nitrogen experiments (Table 2).

Relationship between A_{net} *and* F_s

For IL-grown *Camelina* plants under acute water deficit, a positive linear relationship was observed between A_{net} and F_s for all the data across treatments and PAR levels ($R^2 = 0.57$; $F_{1,98} = 131.95$; $P \leq 0.01$). The slopes of A_{net}/F_s were different between treatments ($F_{2,93} = 8.33$; $P < 0.01$), as were the intercepts ($F_{2,95} = 24.73$; $P \leq 0.01$; Fig. 5*a*). Pairwise comparison of slopes showed that control and re-watered plants had steeper A_{net}/F_s relationships compared with water-deficit treated plants (Fig. 5*a*). Further, when the average of A_{net} and F_s across all PAR levels per each water treatment was computed, A_{net} was able to differentiate the three water treatments ($P \leq 0.05$), whereas F_s was not significantly different between treatments (Fig. 5*b*). It is important to note that only at PAR levels between 300 and 500 µmol m^{-2} s^{-1} a clear nitrogen trend was distinguishable. The highest correlation coefficients for the linear regression between A_{net} and F_s was observed at PAR 300 µmol m^{-2} s^{-1} ($R^2 = 0.79$). The regressions between A_{net} and F_s for other PAR levels, below 300 and above 500 µmol m^{-2} s^{-1}, were not significant ($P > 0.05$).

Table 2. Results of the repeated-measures ANOVA *F*-test comparing effects of watering (well watered, water-deficit, and re-water) and nitrogen treatment (low, medium, and high nitrogen) on leaf-level gas-exchange and fluorescence parameters

Significant effects are indicated: *, $P \leq 0.05$; **, $P \leq 0.01$; ns, not significant at $P < 0.05$ (*F*-test degrees of freedom)

Parameter	Treatment	
	$Camelina_{(2,8)}$	$Wheat_{(2,6)}$
g_s	9.66**	1.50ns
A_{net}	20.6**	16.2**
ETR	22.1**	4.68ns
F_s	0.28ns	21.3**
F_0	1.53ns	1.7E+31**
F_s/F_0	1.46ns	0.78ns
F_v/F_m	2.04ns	6.7E+29**
PQ	7.41*	1.03ns
NPQ	5.18*	0.08ns

Similarly, for HL-grown wheat plants under chronic nitrogen deficit, a weak positive correlation was found between A_{net} and F_s for all the data across treatments and PAR levels ($R^2 = 0.11$; $F_{1,80} = 9.51$; $P < 0.01$). Unlike *Camelina* no differences were observed between treatments in the slope ($F_{2,75} = 0.53$; $P > 0.5$) or intercepts ($F_{2,77} = 0.47$; $P > 0.5$) of the obtained relationships (Fig. 6*a*). However, the average of both A_{net} and F_s for plants under high and medium fertilisation rate differed significantly compared with low fertilisation plants (Fig. 6*b*). Like IL-grown *Camelina*, at the light level at which plants were grown, higher values of A_{net} and F_s corresponded to high and medium nitrogen rates and lower values corresponded to plants under nitrogen deficit (Fig. 6*d–j*). A strong and significant ($P < 0.01$) correlation between A_{net} and F_s was observed over a broader PAR range (100–1800 µmol m^{-2} s^{-1}). Notably, only when PAR reached the light compensation point (PAR = 100 µmol m^{-2} s^{-1}), A_{net} differentiated nitrogen treatments; and a strong correlation between A_{net} and F_s was found. The highest correlation coefficients for the linear regression between A_{net} and F_s was observed at PAR 500 µmol m^{-2} s^{-1} ($R^2 = 0.92$). Again, F_s/F_0 did not improve the correlation either for the water or nitrogen experiment; indeed, weaker correlations were found between A_{net} and F_s/F_0 than between A_{net} and F_s from PAR 100 to1800 µmol m^{-2} s^{-1} for wheat ($R^2 < 0.35$) (data not shown).

Discussion

The results of this study confirm that F_s is able to track variations in photosynthetic capacity in response to water stress and nutrient deficit in *Camelina* and wheat plants respectively. We note that the stress signal (decrease in photosynthesis) was found to modulate ChlF via different mechanisms depending on the treatment: (i) by the action of NPQ in response to water stress in *Camelina* plants, or (ii) through the modulation in leaf chlorophyll concentration in response to nitrogen deficit in wheat. Our study demonstrates that the PAR level at which plants were grown was optimum for detecting water and nutrient deficit with F_s. A positive relationship was found between F_s and A_{net} at PAR level at which plants were grown.

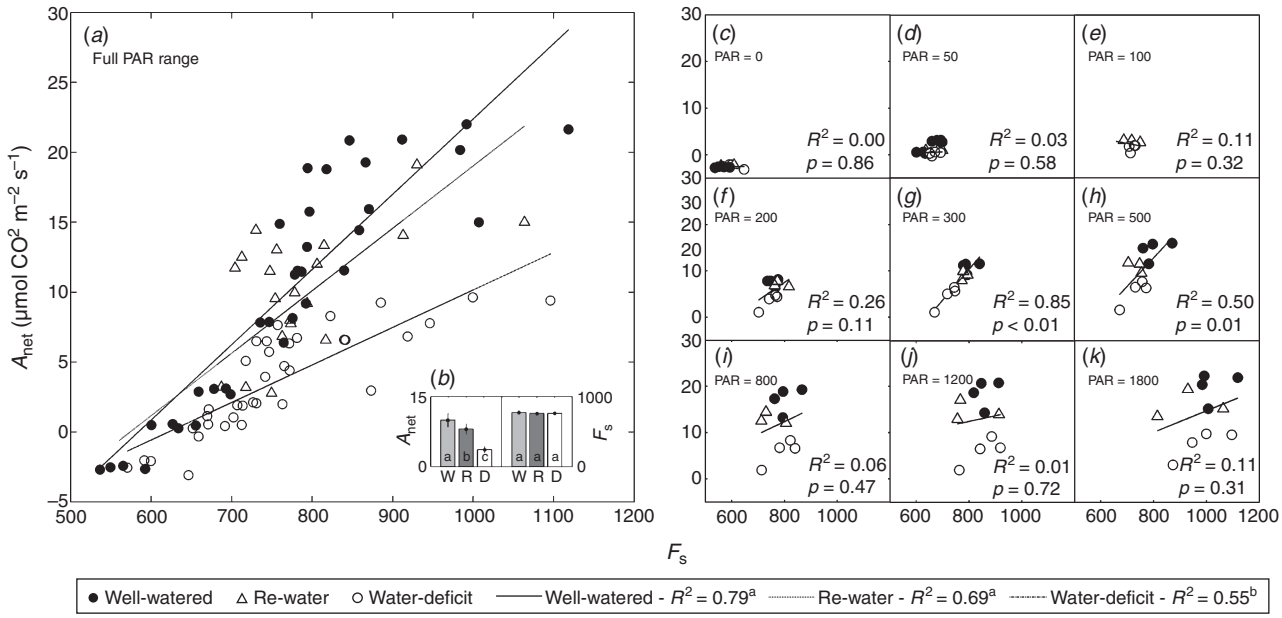

Fig. 5. Experiment I: Intermediate-light history and water deficit. Relationship between net CO_2 assimilation (A_{net}) and steady-state fluorescence (F_s) in *Camelina* plants under well watered conditions (closed circles), after 8 days without watering (water-deficit, open circles), and 1 day after being re-watered (open triangles). (*a*) A_{net} vs F_s across the full PAR range ($P \leq 0.05$). Different letters after R^2 denote significantly different regression lines at $P \leq 0.05$ (ANOVA). (*b*) A_{net} and F_s average rate across all PAR level per each water treatment, where W is well-watered, R is re-watering and D is water-deficit. Different letters denote significant differences at the $P \leq 0.05$. Values are means ± s.e. ($n = 36$). (*c–k*) A_{net} vs F_s at a PAR level of 0, 50, 100, 200, 300, 500, 800, 1200 and 1800 μmol m^{-2} s^{-1}.

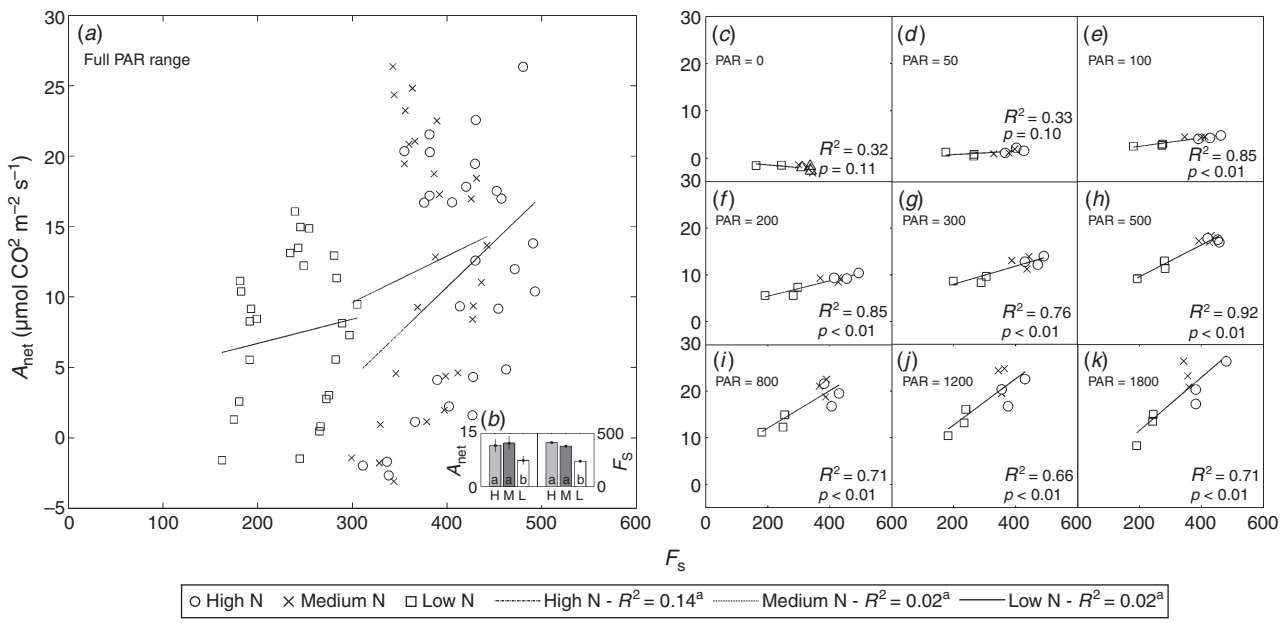

Fig. 6. Experiment II: High-light history and nitrogen deficit. Relationship between net CO_2 assimilation (A_{net}) and steady-state fluorescence (F_s) in wheat plants under high-nitrogen (open circles), medium-nitrogen (cross), and low-nitrogen conditions (open square). (*a*) A_{net} vs F_s across the full PAR ranges. Different letters after R^2 denote significantly different regression lines at $P \leq 0.05$ (ANOVA). (*b*) A_{net} and F_s average rate across all PAR level per each nitrogen treatment, where H is high nitrogen, M is medium nitrogen, and L is low nitrogen. Different letters denote significant differences at the $P \leq 0.05$. Values are means ± s.e. ($n = 27$) (*c–k*) A_{net} vs F_s at a PAR level of 0, 50, 100, 200, 300, 500, 800, 1200 and 1800 μmol m^{-2} s^{-1}.

Plants have evolved active mechanisms to adjust A_{net}, and NPQ but not F_s. F_s is a de-excitation residual of the light not used for photosynthesis or dissipated thermally. A_{net} is mainly controlled by light and CO_2 availability. Under increasing PAR conditions A_{net} saturates (Figs 3*d*, 4*d*). Light capture and electron transport tend to increase linearly with PAR but the capacity for CO_2 assimilation by the Calvin-Benson cycle depends on independent factors such as internal CO_2 concentration (regulated via stomata conductance and overall water availability). When PAR increases, excess energy accumulates, as the rate of light energy captured in the photosystems exceeds the rate of energy consumption by the Calvin-Benson cycle (Müller *et al*. 2001; Ensminger *et al*. 2006). Excess energy can be harmlessly dissipated via regulated thermal energy dissipation or NPQ, as well as other alternative energy pathways such as photorespiration (Müller *et al*. 2001; Porcar-Castell *et al*. 2014).

In contrast, the rapidly reversible NPQ quenching is largely controlled by the xanthophyll-cycle and protonation of specific photosystem proteins (Müller *et al*. 2001; Demmig-Adams and Adams 2006) with the maximum capacity of NPQ proportional to the growth light environment (Serôdio and Lavaud 2011). Therefore, any stress factor that reduces the performance of photosynthesis in terms of A_{net} is expected to translate into an increase in NPQ and consequently a decrease in F_s (Fig. 3*d–f* and Fig. 4*d–f*; Flexas and Medrano 2002).

Our study corroborates that growing light conditions define the maximum capacity of NPQ to dissipate the excess of energy. For IL-grown plants NPQ drastically increase at growing PAR levels (300–500 $\mu mol\, m^{-2}\, s^{-1}$) and for HL-grown plants NPQ presented a linear increase with PAR (Figs 3*e*, 4*e*). Accordingly, under growing light conditions and modulated by the action of NPQ we expected to find a good correlation between F_s and A_{net} for both water and nitrogen experiments. However, NPQ was not always the modulating factor as expected. Depending on the type of stress, different mechanisms were found to explain this relationship, NPQ in response to water stress and chlorophyll concentration in response to nitrogen deficit.

For IL-grown *Camelina*, water deficit induced changes in NPQ, and thus, also in F_s, but only at growing-light conditions, PAR 300 to 500 $\mu mol\, m^{-2}\, s^{-1}$. Under acute water deficit, stomata close, limiting CO_2 availability in the chloroplast, reducing A_{net} and CO_2/O_2 ratios (Flexas et al. 1999). Increased O_2 uptake potential under reduced CO_2 assimilation has been ascribed to either oxygenase activity or electron transport to O_2 through a Mehler type reaction. The Mehler reaction, linked to the ascorbate pathway, uses electrons without consuming ATP (Asada 1999), thus, increasing trans-thylakoid ΔpH (Schreiber and Neubauer 1990). The increase *in trans*-thylakoid ΔpH mediates xanthophyll de-epoxidation, which increases rapidly the reversible NPQ quenching (Gilmore 1997). Additionally, the increase in NPQ when PAR >300 $\mu mol\, m^{-2}\, s^{-1}$ may be due to the regulation of the PSII quantum yield thought the cyclic electron flow (CEF). The CEF protect the PSII from photoinhibitation because of its generation of ΔpH across the thylakoids membranes for NPQ formation (Makino *et al.* 2002; Kou *et al.* 2013). Under growth-light conditions, thermal energy dissipation is within its dynamic range (i.e. operative but not saturated) and therefore it is sensitive to changes in A_{net}. In turn, F_s was also sensitive to stress via NPQ (Fig. 5*g*, *h*).

However, nitrogen deficit for wheat did not induce significant differences in NPQ between treatments (Fig. 4*e*). Nitrogen availability is known to be positively correlated with leaf chlorophyll concentrations (Niinemets *et al*. 1999). In present study, under low nitrogen treatment NAOC levels were significantly lower than medium-high nitrogen treatments. In turn, leaf chlorophyll content modulates light absorption and consequently A_{net} and F_s as described by Buschmann (2007). Therefore, it is reasonable to expect that the sustained differences in F_s observed between treatments in wheat were caused by differences in leaf pigment concentrations and overall changes in light absorption independent of NPQ.

The similarity between the NPQ and F_s *Camelina* light curves presented in this study for IL-grown and water deficit plants, and the ones from Flexas and Medrano (2002) for grapevines (*Vitis vinifera*) also exposed to water deficit but HL-grown, suggest that a similar response would be found in other species when water is the limiting factor. We note that Flexas and Medrano (2002) reported that NPQ did not reach saturation because plants were grown outdoors. That may suggest that NPQ will not saturate in the field, and therefore, F_s will match the A_{net} response with water deficit over a larger PAR range. On the other hand, the NPQ light curves presented by Verhoeven *et al*. (1997) for spinach plants (*Spinacia oleracea* cv. Nobel) IL-grown with nitrogen deficit, disagreed with the NPQ wheat light curves presented in this study with nitrogen deficit but HL-grown. Verhoeven *et al*. (1997) reported NPQ curves that were statistically different between treatments; however, no F_s light curves were published. To our knowledge, no other study has shown the relationship between A_{net}, NPQ, and F_s light curves when nitrogen is the limiting factor. Therefore, further studies are needed to confirm our results in a broad range of species.

Furthermore, although for both experiments a linear relationship was observed between A_{net} and F_s for all data across treatment and PAR levels (Figs 5*a*, 6*a*), when all light levels were taken into account a consistent mechanism to detect stress was not found. For *Camelina*, the slope of A_{net}/F_s was different between treatments (Fig. 5*a*); however, in our wheat experiment, this was not the case (Fig. 6*a*). However, for field-grown wheat, the average of F_s across all PAR levels was significantly different between treatments (Fig. 6*b*), in contrast to results with *Camelina* (Fig. 5*b*). Therefore, an optimum irradiance level for detecting water and nutrient deficit with F_s should be defined. For IL-grown *Camelina*, F_s between $300 < PAR < 500\ \mu mol\, m^{-2}\, s^{-1}$, could differentiate watering treatments (Fig. 3*f*). For HL-grown wheat, F_s differentiated nitrogen treatments across a broad PAR range ($100 < PAR < 1800\ \mu mol\, m^{-2}\, s^{-1}$; Fig. 4*f*). For both experiments the prevailing PAR level at which the plants were grown was within the optimum irradiance for detecting stress with F_s (or slightly below), suggesting that fluorescence data obtained under field clear sky conditions has potential to become a highly sensible proxy to plant stress.

To apply these findings to canopy-level observations, the differences between active (PAM F_s) and passive (remote

sensed ChlF) as well as vegetation structure (multiple-scattering and re-absorption) needs to be taken into account. F_s is the fluorescence induced by a weak and constant modulated light and therefore represents a fluorescence yield, whereas remote sensed ChlF is the total fluorescence emitted in response to solar illumination. Different models have been designed to simulate the fluorescence signal at the top-of-canopy level, including (i) MD12 (Magnani *et al*. 2014) to capture fundamental processes in the leaf photosynthetic centres linking ChlF with photosynthesis but include limited information regarding leaf and canopy structure, (ii) FluorSAIL (Verhoef 2004) to simulate the leaf reflectance and transmittance along with ChlF signal, but providing an inaccurate simulation of the fluorescence spectral profile which is largely affected by photon re-absorption in leaves and canopy (Malenovsky *et al*. 2009) and (iii) SCOPE (van der Tol *et al*. 2009) to represent an accurate propagation of the fluorescence signals and fluxes to the top of the canopy, but lacking in the integration of fundamental processes. The integration of these three models is key to improving our understanding of top-of-canopy ChlF measurements (Mohammed *et al*. 2014) and for the use of remote sensed ChlF to monitor changes in plant photosynthetic capacity due to light, water or nitrogen limitations.

In order to validate that the results presented in the present study can be used to better understand ChlF changes at canopy level, active (leaf-level) and passive (canopy-level) measurements of ChlF were performed one day after the light curves measurements in Experiment II. To compare both datasets, a representative number of leaves were measured using the active technique and then averaged to a unique value for the canopy. In this study, a significant positive linear relationship was observed between active (leaf level) and passive (canopy level) measurements ($R^2 = 0.60$ and $P < 0.01$, see Fig. S1, available as Supplementary Material to this paper).

Conclusion

This work demonstrates that changes in ChlF under growth PAR conditions can be used as a versatile indicator of crop stress in response to both water and nitrogen deficit. Under acute water deficit, NPQ modulates ChlF and this drives its relationship with A_{net}. In contrast though, when chronic nitrogen deficit is a limiting factor chlorophyll concentration modulates ChlF and its correlation with A_{net}. The results provide support for the use of remotely-sensed ChlF as a proxy to monitor plant stress dynamics from space given that remote sensing of ChlF will be measured under growth light conditions. Future work should focus on studies related to species and structure heterogeneity. More work is also needed to extrapolate our results to a broad range of species and to canopy-level measurements. Finally, it is paramount to assess how the results obtained with PAM fluorometry can be extrapolated and compared with those obtained with remotely sensed sun-induced fluorescence estimated within narrow reflectance bands (Meroni *et al*. 2009; Porcar-Castell *et al*. 2014).

Acknowledgements

The authors are in debt to Dr Michael E Salvucci (USDA-ARS, Maricopa, USA) for expert advice and help that allowed the experimental work conducted. We thank two anonymous reviewers for valuable and constructive comments. This research was supported in part by the NASA Soil Moisture Active Passive (SMAP) Science Definition Team (08-SMAPSDT08–0042) and is a result of a fellowship funded by the USDA OECD Co-operative Research Program. A P-C was funded by the Academy of Finland (Projects # 138884 and 272041).

References

Asada K (1999) The water–water cycle in chloroplasts: scavenging of active oxygens and dissipation of excess photons. *Annual Review of Plant Physiology and Plant Molecular Biology* **50**(1), 601–639. doi:10.1146/annurev.arplant.50.1.601

Baker NR (2008) Chlorophyll fluorescence: a probe of photosynthesis in vivo. *Annual Review of Plant Biology* **59**(1), 89–113. doi:10.1146/annurev.arplant.59.032607.092759

Baker NR, Rosenqvist E (2004) Applications of chlorophyll fluorescence can improve crop production strategies: an examination of future possibilities. *Journal of Experimental Botany* **55**(403), 1607–1621. doi:10.1093/jxb/erh196

Björkman O (1981) Responses to different quantum flux densities. In 'Physiological plant ecology I'. (Eds PDOL Lange, PPS Nobel, PCB Osmond, PDH Ziegler) pp. 57–107. (Springer: Berlin)

Buschmann C (2007) Variability and application of the chlorophyll fluorescence emission ratio red/far-red of leaves. *Photosynthesis Research* **92**(2), 261–271. doi:10.1007/s11120-007-9187-8

Chaves MM (1991) Effects of water deficits on carbon assimilation. *Journal of Experimental Botany* **42**(1), 1–16. doi:10.1093/jxb/42.1.1

Choudhury BJ (2001) Estimating gross photosynthesis using satellite and ancillary data: approach and preliminary results. *Remote Sensing of Environment* **75**(1), 1–21. doi:10.1016/S0034-4257(00)00151-6

Delegido J, Alonso L, González G, Moreno J (2010) Estimating chlorophyll content of crops from hyperspectral data using a normalized area over reflectance curve (NAOC). *International Journal of Applied Earth Observation and Geoinformation* **12**(3), 165–174. doi:10.1016/j.jag.2010.02.003

Demmig-Adams B, Adams WW (1992) Photoprotection and other responses of plants to high light stress. *Annual Review of Plant Physiology and Plant Molecular Biology* **43**(1), 599–626. doi:10.1146/annurev.pp.43.060192.003123

Demmig-Adams B, Adams WW 3rd (2006) Photoprotection in an ecological context: the remarkable complexity of thermal energy dissipation. *New Phytologist* **172**(1), 11–21. doi:10.1111/j.1469-8137.2006.01835.x

Ensminger I, Busch F, Huner NPA (2006) Photostasis and cold acclimation: sensing low temperature through photosynthesis. *Physiologia Plantarum* **126**(1), 28–44. doi:10.1111/j.1399-3054.2006.00627.x

Flexas J, Medrano H (2002) Drought-inhibition of photosynthesis in C_3 plants: stomatal and non-stomatal limitations revisited. *Annals of Botany* **89**(2), 183–189. doi:10.1093/aob/mcf027

Flexas J, Escalona JM, Medrano H (1999) Water stress induces different levels of photosynthesis and electron transport rate regulation in grapevines. *Plant, Cell & Environment* **22**(1), 39–48. doi:10.1046/j.1365-3040.1999.00371.x

Fröhlich A, Rice B (2005) Evaluation of *Camelina sativa* oil as a feedstock for biodiesel production. *Industrial Crops and Products* **21**(1), 25–31. doi:10.1016/j.indcrop.2003.12.004

Gamon JA, Peñuelas J, Field CB (1992) A narrow-waveband spectral index that tracks diurnal changes in photosynthetic efficiency. *Remote Sensing of Environment* **41**(1), 35–44. doi:10.1016/0034-4257(92)90059-S

Gilmore AM (1997) Mechanistic aspects of xanthophyll cycle-dependent photoprotection in higher plant chloroplasts and leaves. *Physiologia Plantarum* **99**(1), 197–209. doi:10.1111/j.1399-3054.1997.tb03449.x

Keck Institute for Space Studies (2013) 'New methods for measurements of photosynthesis from space.' (Keck Institute for Space Studies: Pasadena, CA)

Kou J, Takahashi S, Oguchi R, Fan D-Y, Badger MR, Chow WS (2013) Estimation of the steady-state cyclic electron flux around PSI in spinach leaf discs in white light, CO_2-enriched air and other varied conditions. *Functional Plant Biology* **40**(10), 1018–1028. doi:10.1071/FP13010

Kramer DM, Johnson G, Kiirats O, Edwards GE (2004) New fluorescence parameters for the determination of QA redox state and excitation energy fluxes. *Photosynthesis Research* **79**(2), 209–218. doi:10.1023/B:PRES.0000015391.99477.0d

Krause GH, Weis E (1984) Chlorophyll fluorescence as a tool in plant physiology. *Photosynthesis Research* **5**(2), 139–157. doi:10.1007/BF00028527

Laisk A, Oja V, Rasulov B, Eichelmann H, Sumberg A (1997) Quantum yields and rate constants of photochemical and nonphotochemical excitation quenching (experiment and model). *Plant Physiology* **115**(2), 803–815.

Magnani F, Raddi S, Porcar-Castell A (2014) Modelling photochemistry from seasonal changes in steady-state fluorescence under field conditions in *Pinus sylvestris*. In '5th International Workshop on Remote Sensing of Vegetation Fluorescence'. (European Space Agency (ESA: Paris)

Makino A, Miyake C, Yokota A (2002) Physiological functions of the water–water cycle (Mehler reaction) and the cyclic electron flow around PSI in rice leaves. *Plant & Cell Physiology* **43**(9), 1017–1026. doi:10.1093/pcp/pcf124

Malenovsky Z, Mishra KB, Zemek F, Rascher U, Nedbal L (2009) Scientific and technical challenges in remote sensing of plant canopy reflectance and fluorescence. *Journal of Experimental Botany* **60**(11), 2987–3004. doi:10.1093/jxb/erp156

Martin EC (2007) Arizona irrigation scheduling system (AZSched). Available at http://ag.arizona.edu/crop/irrigation/azsched/azsched.html [Verified 30 April 2015]

Meroni M, Rossini M, Guanter L, Alonso L, Rascher U, Colombo R, Moreno J (2009) Remote sensing of solar-induced chlorophyll fluorescence: Review of methods and applications. *Remote Sensing of Environment* **113**(10), 2037–2051. doi:10.1016/j.rse.2009.05.003

Mohammed G, Goulas Y, Magnani F, Moreno J, Olejníčková J, Rascher U, van der Tol C, Verhoef W, Ač A, Daumard F, Galle A, Malenovský Z, Pernokis D, Rivera JP, Verrelst J, Drusch M (2014) 2012 FLEX/Sentinel-3 tandem mission photosynthesis study. Final report no. ESTEC Contract no. 4000106396/12/NL/AF.

Müller P, Li X-P, Niyogi KK (2001) Non-photochemical quenching. A response to excess light energy. *Plant Physiology* **125**(4), 1558–1566. doi:10.1104/pp.125.4.1558

Niinemets U, Kull O, Tenhunen JD (1999) Variability in leaf morphology and chemical composition as a function of canopy light environment in coexisting deciduous trees. *International Journal of Plant Sciences* **160**(5), 837–848. doi:10.1086/314180

Porcar-Castell A (2011) A high-resolution portrait of the annual dynamics of photochemical and non-photochemical quenching in needles of *Pinus sylvestris*. *Physiologia Plantarum* **143**(2), 139–153. doi:10.1111/j.1399-3054.2011.01488.x

Porcar-Castell A, Garcia-Plazaola JI, Nichol CJ, Kolari P, Olascoaga B, Kuusinen N, Fernández-Marín B, Pulkkinen E, Nikinmaa E (2012) Physiology of the seasonal relationship between the photochemical reflectance index and photosynthetic light use efficiency. *Oecologia* **170**(2), 313–323. doi:10.1007/s00442-012-2317-9

Porcar-Castell A, Tyystjärvi E, Atherton J, van der Tol C, Flexas J, Pfündel E, Moreno J, Frankenberg C, Berry JA (2014) Linking chlorophyll-a fluorescence to photosynthesis for remote sensing applications: mechanisms and challenges. *Journal of Experimental Botany* **65**(15), 4065–4095. doi:10.1093/jxb/eru191

Rawson HM, Gómez Macpherson H (2000) 'Irrigated wheat: managing your crop.' (FAO: Rome)

Rosema A, Snel JFH, Zahn H, Buurmeijer WF, Van Hove LWA (1998) The relation between laser-induced chlorophyll fluorescence and photosynthesis. *Remote Sensing of Environment* **65**(2), 143–154. doi:10.1016/S0034-4257(98)00020-0

Schreiber U, Neubauer C (1990) O_2-dependent electron flow, membrane energization and the mechanism of non-photochemical quenching of chlorophyll fluorescence. *Photosynthesis Research* **25**(3), 279–293. doi:10.1007/BF00033169

Serôdio J, Lavaud J (2011) A model for describing the light response of the nonphotochemical quenching of chlorophyll fluorescence. *Photosynthesis Research* **108**(1), 61–76. doi:10.1007/s11120-011-9654-0

Stylinski C, Gamon J, Oechel W (2002) Seasonal patterns of reflectance indices, carotenoid pigments and photosynthesis of evergreen chaparral species. *Oecologia* **131**(3), 366–374. doi:10.1007/s00442-002-0905-9

Tyner EH, Webb JR (1946) The relation of corn yields to nutrient balance as revealed by leaf analysis. *Agronomy Journal* **38**(2), 173–185. doi:10.2134/agronj1946.00021962003800020008x

van der Tol C, Verhoef W, Rosema A (2009) A model for chlorophyll fluorescence and photosynthesis at leaf scale. *Agricultural and Forest Meteorology* **149**(1), 96–105. doi:10.1016/j.agrformet.2008.07.007

Verhoef W (2004) Extension of SAIL to model solar-induced canopy fluorescence spectra. In 'Proceedings of 2nd International Workshop on Remote Sensing of Vegetation Fluorescence, Saint-Hubert, Canada'.

Verhoeven AS, Demmig-Adams B, Adams WW (1997) Enhanced employment of the xanthophyll cycle and thermal energy dissipation in spinach exposed to high light and N stress. *Plant Physiology* **113**(3), 817–824.

Verma S, Sellers P, Walthall C, Hall F, Kim J, Goetz S (1993) Photosynthesis and stomatal conductance related to reflectance on the canopy scale. *Remote Sensing of Environment* **44**(1), 103–116. doi:10.1016/0034-4257(93)90106-8

Zar JH (1974) 'Biostatistical analysis.' (Prentice Hall: Englewood Cliffs, NJ, USA)